

OVERVIEW OF STRANGENESS NUCLEAR PHYSICS

AVRAHAM GAL

Racah Institute of Physics, The Hebrew University, Jerusalem 91904, ISRAEL

Selected topics in Strangeness Nuclear Physics are reviewed: Λ -hypernuclear spectroscopy and structure, multistrangeness, and \bar{K} mesons in nuclei.

Keywords: hypernuclei, multistrangeness, \bar{K} mesons nuclear interactions

1. Introduction

The properties of hypernuclei reflect the nature of the underlying baryon-baryon interactions and, thus, can provide tests of models for the free-space hyperon-nucleon (YN) and hyperon-hyperon (YY) interactions. The Nijmegen group has constructed a number of meson-exchange, soft-core models, using $SU(3)_F$ symmetry to relate coupling constants and form factors.¹ The Jülich group, in addition to YN meson exchange models,² published recently leading-order chiral effective-field theory YN and YY potentials.³ Quark models have also been used within the $(3q) - (3q)$ resonating group model (RGM), augmented by a few effective meson exchange potentials of scalar and pseudoscalar meson nonets directly coupled to quarks.⁴ Finally, we mention recent lattice QCD calculations.^{5,6}

On the experimental side, there is a fair amount of data on single- Λ hypernuclei, including production, structure and decay modes.⁷ Little is known on strangeness $S=-2$ hypernuclei. The missing information is vital for extrapolating into strange hadronic matter, for both finite systems and in bulk, and into neutron stars.⁸ Therefore, following a brief review of single- Λ hypernuclei in Sect. 2, and even a briefer review of Σ -hyperon nuclear interactions in Sect. 3, I discuss in Sect. 4 the onset of hyperon nuclear binding, through which the strength of YN and YY interactions may be determined; and aspects of \bar{K} nuclear interactions in Sect. 5, highlighting the issue of kaon condensation. As for the list of references at the very end, many of the recent ones require adding ‘and references cited therein’.

2. Λ Hypernuclei

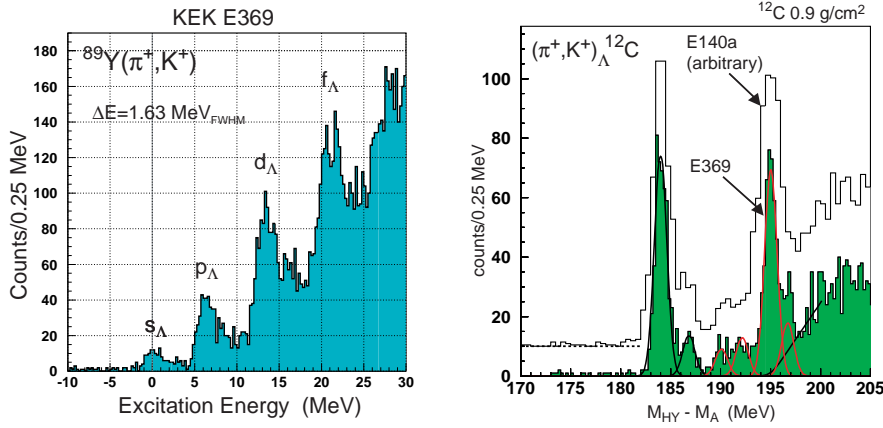


Fig. 1. (π^+, K^+) spectra of Λ hypernuclei, from Ref.¹²

To test YN models against the considerable body of information on Λ hypernuclei, effective interactions for use in limited spaces of shell-model orbits must be evaluated. The Λ well depth resulting from soft-core Nijmegen nuclear-matter G -matrices^{1,9} can be brought to a reasonable agreement with the empirical value 28 MeV deduced in fitting binding energies of Λ single-particle (s.p.) states.¹⁰ However, the partial-wave contributions, in particular the spin dependence of the central interaction, vary widely in different models, and the Λ -nuclear spin-orbit splitting does not come sufficiently small in any of the published models^a. Figure 1 shows examples of Λ s.p. peak structures in $^{89}_{\Lambda}\text{Y}$ and in $^{12}_{\Lambda}\text{C}$. Although the splitting of the f_{Λ} orbit in $^{89}_{\Lambda}\text{Y}$ may suggest a spin-orbit splitting of 1.7 MeV, a more careful shell-model analysis shows that it is consistent with a Λ spin-orbit splitting of merely 0.2 MeV, with most of the observed splitting due to mixing of different ΛN^{-1} particle-hole excitations.¹³ Interesting hypernuclear structure is also revealed between major Λ s.p. states in $^{12}_{\Lambda}\text{C}$. This has not been studied yet with sufficient resolution in medium-weight and heavy hypernuclei, but data already exist from JLab on ^{12}C and other targets,

^aNevertheless, it was suggested recently that missed $\Lambda \rightarrow \Sigma \rightarrow \Lambda$ iterated one-pion exchange contributions cancel out the short-range $\sigma + \omega$ mean-field normal contributions to the Λ nuclear spin-orbit potential.¹¹

with sub-MeV resolution, as shown in this Symposium by Garibaldi and Tang. Furthermore, even with the coarser resolution of the (π^+, K^+) data shown in Fig. 1, most of the $^{12}_{\Lambda}\text{C}$ levels between the (left) $1s_{\Lambda}$ peak and the (right) $1p_{\Lambda}$ peak are particle-stable and could be studied by looking for their electromagnetic cascade deexcitation to the ground state.

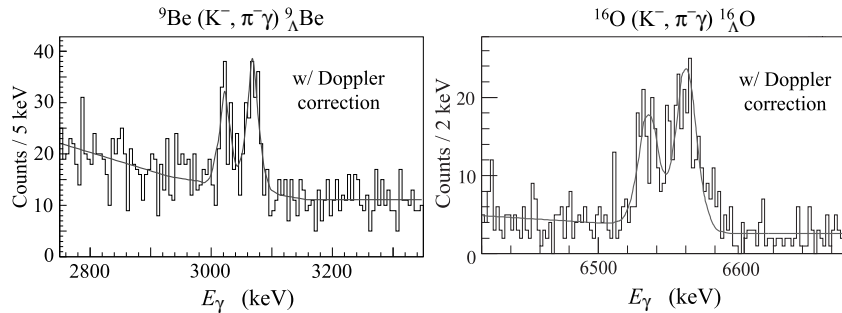


Fig. 2. γ -ray spectra of Λ hypernuclei from BNL-E930, see Tamura's review.¹⁴ The observed twin peaks (in order left to right) result from the $\frac{5}{2}^+$ and $\frac{3}{2}^+$ levels in $^9_{\Lambda}\text{Be}$ separated by 43 keV, deexciting to the ground state, and from deexcitation of a 1^{-*} level in $^{16}_{\Lambda}\text{O}$ to the ground-state doublet 0^- and 1^- levels separated by 26 keV.

A systematic program of γ -ray measurements has been carried out for light Λ hypernuclei at BNL and KEK¹⁴ following a proposal made long time ago by Dalitz and Gal,¹⁵ in order to study the spin dependence of the *effective* ΛN interaction in the nuclear p shell,

$$V_{\Lambda N} = \bar{V} + \Delta \vec{s}_N \cdot \vec{s}_{\Lambda} + S_{\Lambda} \vec{l}_N \cdot \vec{s}_{\Lambda} + S_N \vec{l}_N \cdot \vec{s}_N + T S_{12}, \quad (1)$$

specified in terms of four radial matrix elements: Δ for spin-spin, S_{Λ} and S_N for spin-orbit, T for the tensor interaction. The most completely studied hypernucleus to date is $^7_{\Lambda}\text{Li}$ with five observed γ -ray transitions, allowing a good determination of these parameters in the beginning of the p shell:¹⁶

$$A = 7, 9: \quad \Delta = 430, S_{\Lambda} = -15, S_N = -390, T = 30 \text{ (keV)}. \quad (2)$$

The dominant contributions to $^7_{\Lambda}\text{Li}$ level spacings are due to Δ for $1s_{\Lambda}$ inter-doublet spacings, and S_N for intra-doublet spacings (c.f. Table 1).

A remarkable experimental observation of minute doublet spin splittings in $^9_{\Lambda}\text{Be}$ and in $^{16}_{\Lambda}\text{O}$ is shown in Fig. 2. The contributions of the various spin-dependent components of the effective ΛN interaction to these doublet splittings are given in Table 1 using Eq. (2) for $^9_{\Lambda}\text{Be}$ and a somewhat revised

parameter set for heavier hypernuclei, in the $p_{\frac{1}{2}}$ subshell, which exhibit greater sensitivity to the tensor interaction:¹⁶

$$A = 15, 16 : \quad \Delta = 315, S_{\Lambda} = -15, S_N = -350, T = 23.2 \text{ (keV)}. \quad (3)$$

Listed also are calculated $\Lambda\Sigma$ mixing contributions, as detailed in Ref.¹⁶ Very small core polarization contributions bounded by 10 keV are not listed. In ${}^9_{\Lambda}\text{Be}$, since both Δ and T are well controlled by data from other systems, it is fair to state that the observed 43 ± 5 keV doublet splitting provides a stringent measure of the smallness of the Λ spin-orbit term in Λ hypernuclei, consistently with the small $p_{\frac{1}{2}} - p_{\frac{3}{2}}$ Λ spin-orbit splitting associated with the $\Delta E = 152 \pm 54(\text{stat.}) \pm 36(\text{syst.})$ keV splitting observed in ${}^{13}_{\Lambda}\text{C}$.¹⁷

Table 1. Contributions calculated by Millener¹⁶ of $\Lambda\Sigma$ mixing and ΛN spin-dependent interaction terms, Eq. (1), to doublet splittings in ${}^7_{\Lambda}\text{Li}$ and ${}^9_{\Lambda}\text{Be}$ using Eq. (2), and in ${}^{15}_{\Lambda}\text{N}$ and ${}^{16}_{\Lambda}\text{O}$ using Eq. (3), are compared with experiment¹⁴ (in keV).

${}^Z_{\Lambda}A$	J_{upper}	J_{lower}	$\Lambda\Sigma$	Δ	S_{Λ}	S_N	T	$\Delta E_{\text{calc.}}$	$\Delta E_{\text{exp.}}$
${}^7_{\Lambda}\text{Li}$	$\frac{3}{2}^+$	$\frac{1}{2}^+$	72	628	-1	-4	-9	693	691.7 ± 1.2
${}^9_{\Lambda}\text{Be}$	$\frac{3}{2}^+$	$\frac{5}{2}^+$	-8	-14	37	0	28	44	43 ± 5
${}^{15}_{\Lambda}\text{N}$	$\frac{1}{2}^+$	$\frac{3}{2}^+$	42	232	34	-8	-208	92	
${}^{16}_{\Lambda}\text{O}$	1^-	0^-	-29	-117	-21	1	183	27	26.4 ± 1.7

The spin dependence of the ΛN interaction may also be studied by observing pionic weak-decay spectra, as reported in this Symposium by Botta for the FINUDA Collaboration.¹⁸ In particular, the ${}^{15}_{\Lambda}\text{N} \rightarrow \pi^- + {}^{15}\text{O}$ measured spectrum suggests a spin-parity assignment $J^{\pi}({}^{15}_{\Lambda}\text{N}_{\text{g.s.}}) = \frac{3}{2}^+$, consistently with the positive value predicted by Millener¹⁶ for the ground-state doublet splitting $E(\frac{1}{2}^+) - E(\frac{3}{2}^+)$ listed in Table 1.

3. Σ hyperons

A vast body of reported (K^-, π^{\pm}) and (π^-, K^+) spectra indicate a repulsive Σ nuclear potential, with a substantial isospin dependence¹⁹ which for very light nuclei may conspire in selected configurations to produce Σ hypernuclear quasibound states, as shown on the left-hand side (l.h.s.) of Fig. 3 for ${}^4_{\Sigma}\text{He}$.^b These data, including recent (π^-, K^+) spectra²⁴ and related DWIA analyses,²⁵ suggest that Σ hyperons do not bind in heavier nuclei.

^bThe discovery of ${}^4_{\Sigma}\text{He}$, in K^- capture at rest, is due to Hayano *et al.*²³

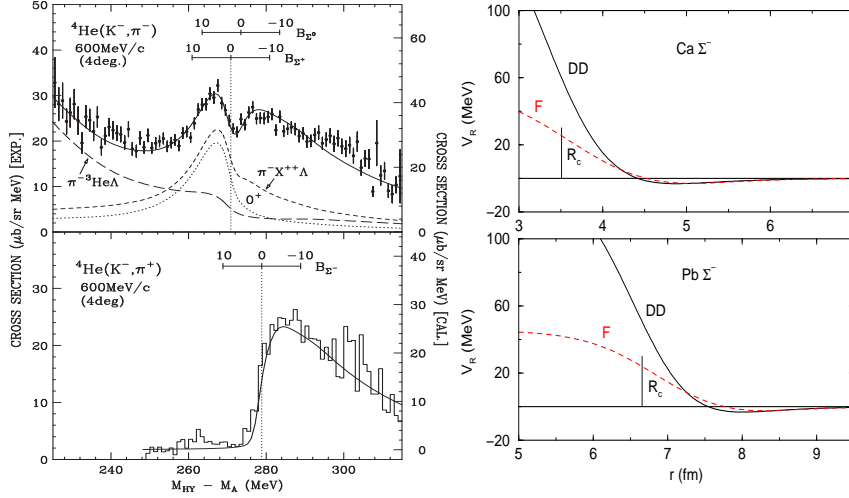


Fig. 3. Left: ${}^4\text{He}(K^-, \pi^\pm)$ spectra, as measured²⁰ and as calculated by Harada,²¹ providing evidence for a ${}^4_\Sigma I = 1/2$ quasibound state in the π^- channel, with binding energy $B_{\Sigma^+} = 4.4 \pm 0.3 \pm 1$ MeV and width $\Gamma = 7.0 \pm 0.7^{+1.2}_{-0.0}$ MeV. Right: $\text{Re } V_{\text{opt}}^\Sigma$ fitted to *all* Σ^- atomic data, for two density-dependent potential models.²² The half-density nuclear charge radius R_c is indicated.

A repulsive component of the Σ nuclear potential is also revealed in analyses of strong-interaction level shifts and widths in Σ^- atoms, as shown on the right-hand side (r.h.s.) of Fig. 3. In fact, $\text{Re } V_{\text{opt}}^\Sigma$ is attractive at low densities outside the nucleus, as enforced by the observed ‘attractive’ Σ^- atomic level shifts, changing into repulsion well outside of the nuclear radius. The precise magnitude and shape of the repulsive component within the nucleus, however, are model dependent.²² The slightly preferred potential F yields $\text{Re } V_{\text{opt}}^\Sigma(\rho_0) \sim 40 - 50$ MeV, roughly consistent with Refs.²⁵ This bears interesting consequences for the balance of strangeness in the inner crust of neutron stars, primarily by delaying the appearance of Σ^- hyperons to higher densities, as shown on the l.h.s. of Fig. 5 in Sect. 4.

The G -matrices constructed from Nijmegen soft-core potential models generally do not produce Σ repulsion in symmetric nuclear matter, as demonstrated in Table 2 using the parametrization

$$V^Y = V_0^Y + \frac{1}{A} V_1^Y \mathbf{T}_A \cdot \mathbf{t}_Y . \quad (4)$$

In contrast to the published Nijmegen soft-core attractive potentials, SU(6) quark-model RGM calculations⁴ in which a strong Pauli repulsion appears in the $I = 3/2$, ${}^3S_1 - {}^3D_1$ ΣN channel give repulsion, and so does an SU(3)

Table 2. Isoscalar and isovector hyperon potentials, Eq. (4) in MeV, calculated for Nijmegen soft-core potential models,^{1,26} denoted by year and version, at nuclear-matter density ($k_F = 1.35 \text{ fm}^{-1}$). The ESC06 results are preliminary. The ESC* models assume specifically repulsive medium modifications affecting weakly the isovector potentials. Excluded are $\text{Im } V^\Sigma$ due to $\Sigma N \rightarrow \Lambda N$ and $\text{Im } V^\Xi$ due to $\Xi N \rightarrow \Lambda \Lambda$.

	97f	04a	04a*	04d	04d*	06d	06d*	phenom.	Ref.
V_0^Λ	-31.7	-38.5	-30.6	-44.1	-37.2	-44.5	-37.5	-28	10
V_0^Σ	-13.9	-36.5	-27.9	-26.0	-16.6	-1.2	+8.2	10 - 50	22,25
V_1^Σ	-30.4	+21.6		+30.4		+52.6	+55.2	$\approx +80$	27
V_0^Ξ		+15.1		-18.7	-12.1			≈ -14	28
V_1^Ξ		+32.5		+50.9	+51.5				

chiral perturbation calculation²⁹ which yields repulsion of order 60 MeV. Phenomenologically $V_0^\Sigma > 0$ and $V_1^\Sigma > 0$, as listed in the table, and both components of V^Σ give repulsion in nuclei. However, given a nuclear core with $(N - Z) < 0$ and owing to the small value of A in ${}^4_\Sigma\text{He}$, the isovector term provides substantial attraction towards binding this exceptional hypernucleus ${}^4_\Sigma\text{He}$, while the isoscalar repulsion reduces the quasibound level width (c.f. Fig. 3).

4. Strangeness binding onset and Strange Hadronic Matter

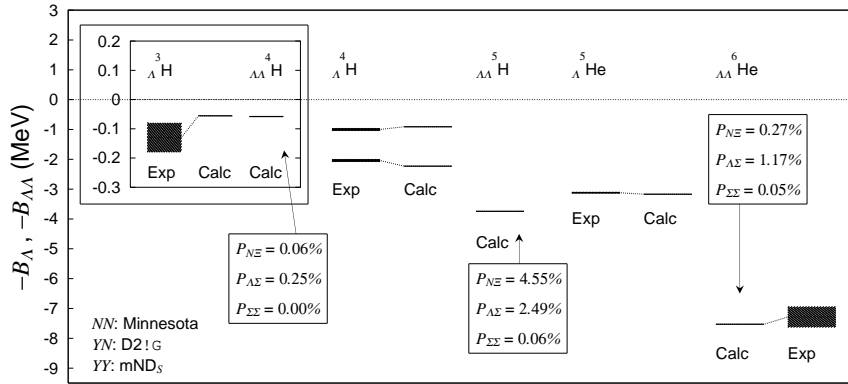


Fig. 4. Λ and $\Lambda\Lambda$ separation energies in s -shell hypernuclei, calculated in Ref.³⁰

Complete few-body calculations of the s -shell hypernuclei, for systems of nucleons and Λ hyperons, with full account of coupled-channel effects due

to the primary $\Lambda N - \Sigma N$ and $\Lambda\Lambda - \Xi N$ mixings, were reported by Nemura *et al.*³⁰ using stochastic variational methods and phenomenological potentials based partly on meson exchange models. The calculated spectra are shown in Fig. 4. In addition to the established ${}^3_\Lambda\text{H}$, ${}^4_\Lambda\text{H} - {}^4_\Lambda\text{He}$ and ${}^5_\Lambda\text{He}$ single- Λ hypernuclei, ${}_{\Lambda\Lambda}{}^4\text{H}$ and ${}_{\Lambda\Lambda}{}^5\text{H} - {}_{\Lambda\Lambda}{}^5\text{He}$ bound states were predicted by fitting to $\Delta B_{\Lambda\Lambda}({}_{\Lambda\Lambda}{}^6\text{He}) \approx 1$ MeV for the only $\Lambda\Lambda$ hypernucleus uniquely assigned by experiment.³¹ We note that ${}_{\Lambda\Lambda}{}^4\text{H}$ is particle-stable in the calculation of Fig. 4 only by a minute 2 keV; given the uncertainties in the input and in the calculations, ${}_{\Lambda\Lambda}{}^4\text{H}$ could still prove unbound.³² Moreover, the experimental evidence³³ for ${}_{\Lambda\Lambda}{}^4\text{H}$ has been challenged recently.³⁴ In contrast, the particle stability of ${}_{\Lambda\Lambda}{}^5\text{H}$ and ${}_{\Lambda\Lambda}{}^5\text{He}$, which have not yet been discovered, appears theoretically robust.³⁵

Very little is established experimentally on the interaction of Ξ hyperons with nuclei. Inclusive (K^-, K^+) spectra²⁸ on ${}^{12}\text{C}$ yield a somewhat shallow attractive potential, $V^\Xi \approx -14$ MeV, by fitting near the Ξ^- hypernuclear threshold. Of the Nijmegen soft-core potentials listed in Table 2, ESC04d* is the closest one to reproducing the phenomenological potential depth and it gives rise, selectively – owing to its strong spin and isospin dependence, to quasibound Ξ states in several light nuclear targets, beginning with ${}^7\text{Li}$.³⁶ In this model, ${}_{\Xi^0}{}^5\text{He}$ is unbound. For a nuclear-matter width $\Gamma_\Xi = 12.7$ MeV calculated in model ESC04d*, it may not be straightforward to resolve the rich spectroscopy predicted for these light nuclear targets. A ‘day-1’ experiment at J-PARC on a ${}^{12}\text{C}$ target is scheduled soon.³⁷

Ξ hyperons could become stabilized in multi- Λ hypernuclei once the decay $\Xi N \rightarrow \Lambda\Lambda$, which releases ≈ 25 MeV in free space, gets Pauli blocked.^c The onset of Ξ particle-stability would occur for ${}_{\Xi^0\Lambda}{}^6\text{He}$ or for ${}_{\Xi^0\Lambda\Lambda}{}^7\text{He}$, depending on whether or not ${}_{\Xi^0}{}^5\text{He}$ is bound, and by how much (if bound).³⁸ Particle stability for Ξ hyperons becomes robust with few more Λ s, even for as shallow Ξ -nucleus potentials as discussed above. The r.h.s. of Fig. 5 demonstrates that Ξ s can be added to a core of ${}^{56}\text{Ni}$ plus Λ s, reaching as high strangeness fraction as $f_S \equiv -S/A \approx 0.7$ while retaining particle stability. This leads to the concept of Strange Hadronic Matter (SHM) consisting of equal fractions of protons, neutrons, Λ , Ξ^0 and Ξ^- hyperons,³⁹ with $f_S = 1$ as in Strange Quark Matter (SQM). Both SHM and SQM provide macroscopic realizations of strangeness, but SHM is more plausible phenomenologically, whereas SQM is devoid of any experimental datum from which to extrapolate.

^cWith ≈ 80 MeV release in $\Sigma N \rightarrow \Lambda N$, however, Σ hyperons are unlikely to stabilize.

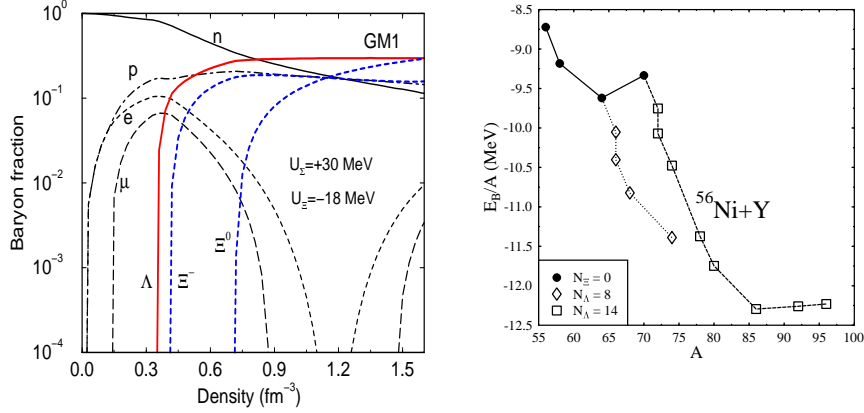


Fig. 5. Left: fractions of baryons and leptons in neutron star matter calculated in RMF with weak YY potentials.⁸ Note that Ξ^- hyperons appear at a density range where Σ^- hyperons would have appeared for an attractive Σ^- nuclear potential. Right: binding energy of ^{56}Ni with added Λ and Ξ hyperons as a function of baryon number A .³⁹ These particle-stable multistrange states decay by weak interactions on a time scale 10^{-10} s.

5. \bar{K} nuclear interactions and \bar{K} condensation

The \bar{K} -nucleus interaction near threshold comes strongly attractive and absorptive in fits to the strong-interaction shifts and widths of K^- -atom levels,²² resulting in deep potentials, $\text{Re } V^{\bar{K}}(\rho_0) \sim -(150 - 200)$ MeV at threshold. Chirally based coupled-channel models that fit the low-energy K^-p reaction data, and the $\pi\Sigma$ spectral shape of the $\Lambda(1405)$ resonance, yield weaker but still very attractive potentials, $\text{Re } V^{\bar{K}}(\rho_0) \sim -100$ MeV, as summarized recently in Ref.⁴⁰ A third class, of relatively shallow potentials with $\text{Re } V^{\bar{K}}(\rho_0) \sim -(40 - 60)$ MeV, was obtained by imposing a Watson-like self-consistency requirement.⁴¹

Table 3. Calculated B_{K^-pp} , mesonic (Γ_m) & nonmesonic (Γ_{nm}) widths.

(MeV)	$\bar{K}NN$ single channel		$\bar{K}NN - \pi\Sigma N$ coupled channels		
	ATMS ⁴²	AMD ⁴³	Faddeev ⁴⁴	Faddeev ⁴⁵	variational ⁴⁶
B_{K^-pp}	48	17 – 23	50 – 70	60 – 95	40 – 80
Γ_m	61	40 – 70	90 – 110	45 – 80	40 – 85
Γ_{nm}	12	4 – 12			~ 20

The onset of nuclear (quasi) binding for K^- mesons occurs already with

just one proton: the $\Lambda(1405)$ which is represented by an S -matrix pole about 27 MeV below the K^-p threshold. However, in chirally based models, the $I = 0$ $\bar{K}N - \pi\Sigma$ coupled channel system exhibits also another S -matrix pole roughly 12 MeV below threshold and it is this pole that enters the effective $\bar{K}N$ interaction, affecting dominantly the \bar{K} -nucleus dynamics.⁴⁰ The distinction between models that consider the twin-pole situation and those that are limited to the $\Lambda(1405)$ single-pole framework shows up already in calculations of $[\bar{K}(NN)_{I=1}]_{I=1/2, J^\pi=0^-}$, loosely denoted K^-pp , which is the configuration that maximizes the strongly attractive $I = 0$ $\bar{K}N$ interaction with two nucleons. In Table 3 which summarizes K^-pp binding-energy calculations, the $I = 0$ $\bar{K}N$ binding input to the ATMS calculation is stronger by about 15 MeV than for the AMD calculation, resulting in almost 30 MeV difference. Furthermore, it is clear from the ‘coupled-channel’ entries in the table that the explicit use of the $\pi\Sigma N$ channel adds about 20 ± 5 MeV to the binding energy calculated using effective $\bar{K}N$ potential within a single-channel calculation. The experimental state of the art in searching for a K^-pp signal was discussed in this Symposium by Yamazaki, and also by Fabbietti (FOPI) and Piano (FINUDA). In view of the wide spectrum of predictions in Table 3, new dedicated experiments are welcome; indeed a ‘day-1’ experiment at J-PARC on a ^3He target is scheduled soon.⁴⁷

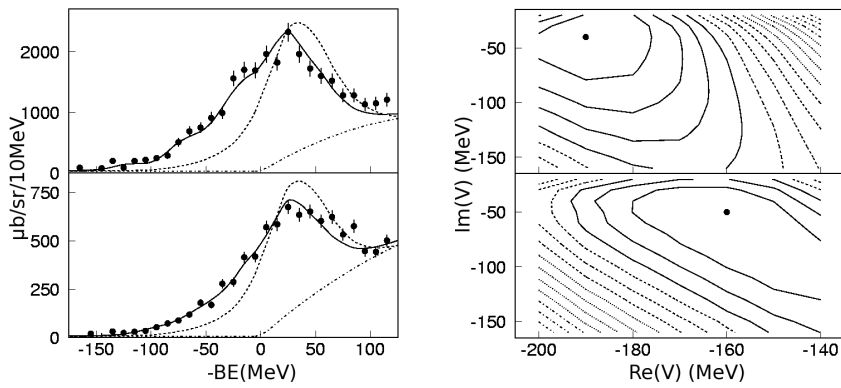


Fig. 6. Missing mass spectra (left) and χ^2 contour plots (right) for the inclusive reactions (K^-, n) (upper) and (K^-, p) (lower) at $p_{K^-} = 1$ GeV/c on ^{12}C , from Ref.⁴⁸

A fairly new and independent evidence in favor of deep \bar{K} -nucleus potentials is provided by (K^-, n) and (K^-, p) spectra⁴⁸ taken at KEK on ^{12}C ,

and very recently also on ^{16}O at $p_{K^-} = 1 \text{ GeV}/c$ (presented in PANIC08). The ^{12}C spectra are shown in Fig. 6, where the solid lines on the left-hand side represent calculations (outlined in Ref.⁴⁹) using potential depths in the range 160 – 190 MeV. The dashed lines correspond to using relatively shallow potentials of depth about 60 MeV which I consider therefore excluded by these data. Although the potentials that fit these data are sufficiently deep to support strongly-bound antikaon states, a fairly sizable extrapolation is required to argue for \bar{K} -nuclear quasibound states at energies of order 100 MeV below threshold, using a potential determined largely near threshold. Furthermore, the best-fit $\text{Im } V^{\bar{K}}$ depths of 40 – 50 MeV imply that \bar{K} -nuclear quasibound states are broad, as studied in Refs.^{50,51}

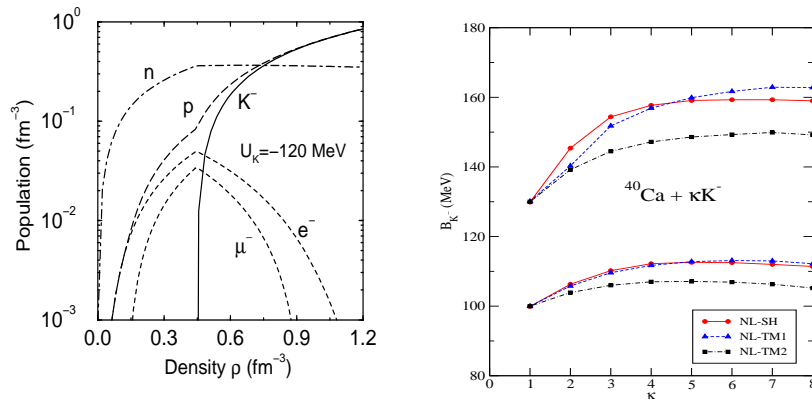


Fig. 7. Left: calculated neutron-star population as a function of nucleon density, from Ref.⁵² The neutron density stays nearly constant once kaons condense. Right: calculated separation energies B_{K^-} in multi- K^- nuclei based on ^{40}Ca as a function of the number κ of K^- mesons in several nuclear RMF models with two choices of parameters fixed for $\kappa = 1$, from Ref.⁵³ See also Mares' talk in this Symposium.

A robust consequence of the sizable \bar{K} -nucleus attraction is that K^- condensation occurs in neutron stars at about 3 times nuclear matter density, as shown on the l.h.s. of Fig. 7. Comparing it with the l.h.s. of Fig. 5, also for neutron stars, but where strangeness materialized through hyperons, one may ask whether or not the r.h.s of Fig. 5, for finite nuclei, also offers an analogy: do \bar{K} mesons condense in nuclear matter? This question was posed and answered, negatively, in Ref.⁵³ calculating multi- \bar{K} nuclear configurations. The r.h.s. of Fig. 7 demonstrates a remarkable saturation of K^- separation energies B_{K^-} calculated in multi- K^- nuclei $^{40}\text{Ca} + \kappa K^-$,

independently of the applied RMF model. The saturation values of B_{K^-} do not allow conversion of hyperons to \bar{K} mesons through the strong decays $\Lambda \rightarrow p + K^-$ or $\Xi^- \rightarrow \Lambda + K^-$ in multi-strange hypernuclei, which therefore remain the lowest-energy configuration for multi-strange systems. This provides a powerful argument against \bar{K} condensation in the laboratory, under strong-interaction equilibrium conditions.⁵³ It does not apply to kaon condensation in neutron stars, where equilibrium configurations are determined by weak-interaction conditions.

Acknowledgments

Thanks are due to John Millener for instructive correspondence on the analysis of the γ -ray experiments, and to the Organizers of SENDAI08 for their gracious hospitality.

References

1. Th.A. Rijken, Y. Yamamoto, *Nucl. Phys. A* **804**, 51 (2008).
2. J. Haidenbauer, U.-G. Meißner, *Phys. Rev. C* **72**, 044005 (2005).
3. H. Polinder, J. Haidenbauer, U.-G. Meißner, *Nucl. Phys. A* **779**, 244 (2006), *Phys. Lett. B* **653**, 29 (2007).
4. Y. Fujiwara, Y. Suzuki, C. Nakamoto, *Prog. Part. Nucl. Phys.* **58**, 439 (2007).
5. S.R. Beane, *et al.* [NPLQCD], *Nucl. Phys. A* **794**, 62 (2007).
6. H. Nemura, N. Ishii, S. Aoki, T. Hatsuda, *Phys. Lett. B* **673**, 136 (2009).
7. O. Hashimoto, H. Tamura, *Prog. Part. Nucl. Phys.* **57**, 564 (2006).
8. J. Schaffner-Bielich, *Nucl. Phys. A* **804**, 309 (2008).
9. Y. Yamamoto, Th.A. Rijken, *Nucl. Phys. A* **804**, 139 (2008).
10. D.J. Millener, C.B. Dover, A. Gal, *Phys. Rev. C* **38**, 2700 (1988); Y. Yamamoto, H. Bandō, J. Žofka, *Prog. Theor. Phys.* **80**, 757 (1988).
11. N. Kaiser, W. Weise, *Nucl. Phys. A* **804**, 60 (2008).
12. H. Hotchi, *et al.* [KEK E369], *Phys. Rev. C* **64**, 044302 (2001).
13. T. Motoba, D.E. Lanskoy, D.J. Millener, Y. Yamamoto, *Nucl. Phys. A* **804**, 99 (2008).
14. H. Tamura, *et al.*, *Nucl. Phys. A* **804**, 73 (2008).
15. R.H. Dalitz, A. Gal, *Ann. Phys.* **116**, 167 (1978).
16. D.J. Millener, *Nucl. Phys. A* **804**, 84 (2008).
17. S. Ajimura, *et al.* [BNL E929], *Phys. Rev. Lett.* **86**, 4255 (2001).
18. M. Agnello, *et al.* [FINUDA], submitted to *Phys. Lett. B*; see also A. Gal, arXiv:0904.1174 [nucl-th].
19. C.B. Dover, D.J. Millener, A. Gal, *Phys. Rept.* **184**, 1 (1989).
20. T. Nagae, *et al.* [BNL E905], *Phys. Rev. Lett.* **80**, 1605 (1998).
21. T. Harada, *Phys. Rev. Lett.* **81**, 5287 (1998).
22. E. Friedman, A. Gal, *Phys. Rept.* **452**, 89 (2007) and earlier; Σ^- atoms: J. Mareš, E. Friedman, A. Gal, B.K. Jennings, *Nucl. Phys. A* **594**, 311 (1995); K^- atoms: E. Friedman, A. Gal, C.J. Batty, *Nucl. Phys. A* **579**, 518 (1994).

23. R.S. Hayano, *et al.*, *Phys. Lett. B* **231**, 355 (1989).
24. H. Noumi, *et al.*, *Phys. Rev. Lett.* **89**, 072301 (2002), **90**, 049902(E) (2003); P.K. Saha, *et al.* [KEK E438], *Phys. Rev. C* **70**, 044613 (2004).
25. M. Kohno, Y. Fujiwara, Y. Watanabe, K. Ogata, M. Kawai, *Prog. Theor. Phys.* **112**, 895 (2004), *Phys. Rev. C* **74**, 064613 (2006); T. Harada, Y. Hirabayashi, *Nucl. Phys. A* **759**, 143 (2005), **767**, 206 (2006).
26. Th.A. Rijken, Y. Yamamoto, *Phys. Rev. C* **73**, 044008 (2006).
27. C.B. Dover, A. Gal, D.J. Millener, *Phys. Lett. B* **138**, 337 (1984).
28. T. Fukuda, *et al.* [KEK E224], *Phys. Rev. C* **58**, 1306 (1998); P. Khaustov, *et al.* [BNL E885], *Phys. Rev. C* **61**, 054603 (2000).
29. N. Kaiser, *Phys. Rev. C* **71**, 068201 (2005).
30. H. Nemura, S. Shinmura, Y. Akaishi, K.S. Myint, *Phys. Rev. Lett.* **94**, 202502 (2005).
31. H. Takahashi, *et al.* [KEK E373], *Phys. Rev. Lett.* **87**, 212502 (2001).
32. I.N. Filikhin, A. Gal, *Phys. Rev. Lett.* **89**, 172502 (2002).
33. J.K. Ahn, *et al.* [BNL E906], *Phys. Rev. Lett.* **87**, 132504 (2001).
34. S.D. Randeniya, E.V. Hungerford, *Phys. Rev. C* **76**, 064308 (2007).
35. I.N. Filikhin, A. Gal, *Nucl. Phys. A* **707**, 491 (2002); K.S. Myint, S. Shinmura, Y. Akaishi, *Eur. Phys. J. A* **16**, 21 (2003); I.N. Filikhin, A. Gal, V.M. Suslov, *Phys. Rev. C* **68**, 024002 (2003).
36. E. Hiyama, Y. Yamamoto, T. Motoba, Th.A. Rijken, M. Kamimura, *Phys. Rev. C* **78**, 054316 (2008); T. Motoba, S. Sugimoto *et al.*, in Proc. PANIC08.
37. T.N. Takahashi, *et al.* [J-PARC E05], in Proc. PANIC08.
38. J. Schaffner, C.B. Dover, A. Gal, C. Greiner, D.J. Millener, H. Stöcker, *Ann. Phys.* **235**, 35 (1994); I.N. Filikhin, A. Gal, *Phys. Rev. C* **65**, 041001(R) (2002); M. Shoeb, Sonika, *J. Phys. G* **36**, 045104 (2009).
39. J. Schaffner, C.B. Dover, A. Gal, C. Greiner, H. Stöcker, *Phys. Rev. Lett.* **71**, 1328 (1993).
40. W. Weise, R. Härtle, *Nucl. Phys. A* **804**, 173 (2008); T. Hyodo, W. Weise, *Phys. Rev. C* **77**, 035204 (2008) and in these Proceedings.
41. A. Ramos, E. Oset, *Nucl. Phys. A* **671**, 481 (2000).
42. T. Yamazaki, Y. Akaishi, *Phys. Lett. B* **535**, 70 (2002).
43. A. Doté, T. Hyodo, W. Weise, *Nucl. Phys. A* **804**, 197 (2008), *Phys. Rev. C* **79**, 014003 (2009) and in these Proceedings.
44. N.V. Shevchenko, A. Gal, J. Mareš, *Phys. Rev. Lett.* **98**, 082301 (2007); N.V. Shevchenko, A. Gal, J. Mareš, J. Révai, *Phys. Rev. C* **76**, 044004 (2007).
45. Y. Ikeda, T. Sato, *Phys. Rev. C* **76**, 035203 (2007), **79**, 035201 (2009).
46. S. Wycech, A.M. Green, *Phys. Rev. C* **79**, 014001 (2009).
47. M. Lio, *et al.* [J-PARC E15&17], in Proc. PANIC08.
48. T. Kishimoto, *et al.* [KEK E548], *Prog. Theor. Phys.* **118**, 181 (2007).
49. J. Yamagata, H. Nagahiro, S. Hirenzaki, *Phys. Rev. C* **74**, 014604 (2006).
50. J. Mareš, E. Friedman, A. Gal, *Phys. Lett. B* **606**, 295 (2005), *Nucl. Phys. A* **770**, 84 (2006).
51. D. Gazda, E. Friedman, A. Gal, J. Mareš, *Phys. Rev. C* **76**, 055204 (2007).
52. N.K. Glendenning, J. Schaffner-Bielich, *Phys. Rev. C* **60**, 025803 (1999).
53. D. Gazda, E. Friedman, A. Gal, J. Mareš, *Phys. Rev. C* **77**, 045206 (2008).